11. D. Pergolesi *et al.*, *Nat. Mater.* **9**, 846–852 (2010).
12. P. Babilo, T. Uda, S. M. Haile, *J. Mater. Res.* **22**, 1322–1330 (2007).
13. P. Babilo, S. M. Haile, *J. Am. Ceram. Soc.* **88**, 2362–2368 (2005).
14. K. D. Kreuer, *Solid State Ion.* **125**, 285–302 (1999).
15. K. D. Kreuer *et al.*, *Solid State Ion.* **145**, 295–306 (2001).
16. M. Shang, J. Tong, R. O'Hayre, *RSC Adv.* **3**, 15769–15775 (2013).
17. J. Tong *et al.*, *J. Membr. Sci.* **203**, 175–189 (2002).
18. K. D. Kreuer, *Annu. Rev. Mater. Res.* **33**, 333–359 (2003).
19. E. Fabbri, D. Pergolesi, E. Traversa, *Chem. Soc. Rev.* **39**, 4355–4369 (2010).
20. D. Poetzsch, R. Merkle, J. Maier, *Phys. Chem. Chem. Phys.* **16**, 16446–16453 (2014).
21. D. Hashimoto, D. Han, T. Uda, *Solid State Ion.* **262**, 687–690 (2014).
22. E. Fabbri, A. Depifanio, E. Dibartolomeo, S. Licoccia, E. Traversa, *Solid State Ion.* **179**, 558–564 (2008).
23. S. Ricote, N. Bonanos, G. Caboche, *Solid State Ion.* **180**, 990–997 (2009).
24. L. Yang *et al.*, *Science* **326**, 126–129 (2009).
25. D. Clark *et al.*, *Phys. Chem. Chem. Phys.* **16**, 5076–5080 (2014).
26. S. Nikodemski, J. Tong, R. O'Hayre, *Solid State Ion.* **253**, 201–210 (2013).
27. I. Luisetto, E. Di Bartolomeo, A. D'Epifanio, S. Licoccia, *J. Electrochem. Soc.* **158**, B1368–B1372 (2011).

ACKNOWLEDGMENTS

This work was supported by Advanced Research Projects Agency–Energy (ARPA-E) for funding under the REBELS program (award DE-AR0000493), the National Science Foundation Materials Research Science and Engineering Centers program under grant DMR-0820518, and the Petroleum Institute in Abu Dhabi, United Arab Emirates. This work is related to U.S. Patent application 62/101,285 (2015) and U.S. Patent application 14/621,091 (2015) filed by J. Tong *et al.* J.T. and R.O'H. developed the intellectual concept, designed all the experiments, and supervised this research. C.D. performed the fabrication and testing experiments of PCFC single cells. M.Sh. synthesized and tested the cathode materials. S.N. identified the copper oxide as an effective sintering aid for solid-state reactive sintering. M.Sa. measured proton concentration in cathode material. S.R. contributed to the preparation of the pastes for the electrolytes and cathode bones. A.A. participated in discussion and analysis of the methane-fueled cell testing. J.T., R.O'H., and C.D. analyzed all experimental data and wrote the paper.

SUPPLEMENTARY MATERIALS

www.sciencemag.org/content/349/6254/1321/suppl/DC1
Materials and Methods
Supplementary Text
Figs. S1 to S24
Tables S1 and S2
References for Fig. 1, A and B
References (*28*–*91*)

21 April 2015; accepted 13 July 2015
Published online 23 July 2015
10.1126/science.aab3987

ORGANIC CHEMISTRY

Site-selective arene C-H amination via photoredox catalysis

Nathan A. Romero, Kaila A. Margrey, Nicholas E. Tay, David A. Nicewicz*

Over the past several decades, organometallic cross-coupling chemistry has developed into one of the most reliable approaches to assemble complex aromatic compounds from preoxidized starting materials. More recently, transition metal–catalyzed carbon-hydrogen activation has circumvented the need for preoxidized starting materials, but this approach is limited by a lack of practical amination protocols. Here, we present a blueprint for aromatic carbon-hydrogen functionalization via photoredox catalysis and describe the utility of this strategy for arene amination. An organic photoredox-based catalyst system, consisting of an acridinium photooxidant and a nitroxyl radical, promotes site-selective amination of a variety of simple and complex aromatics with heteroaromatic azoles of interest in pharmaceutical research. We also describe the atom-economical use of ammonia to form anilines, without the need for prefunctionalization of the aromatic component.

The development of catalytic procedures for the selective modification of carbon-hydrogen (C-H) bonds carries the promise of streamlined and sustainable syntheses of high-value chemicals. Direct transformation of aryl C-H bonds into carbon-carbon (C-C), carbon-oxygen (C-O), and carbon-nitrogen (C-N) bonds can provide efficient access to arenes with diverse structural properties (*1*, *2*). In particular, interest in aryl C-H amination (construction of a C-N bond from a C-H bond) is driven by the ubiquity of aryl C-N bonds in pharmaceuticals, natural products, agrochemicals, pigments, and optoelectronic materials. In contrast to the Buchwald-Hartwig (*3*, *4*) and Chan-Lam (*5*, *6*) aminations, which stand as the current preferred methods for catalytic aryl C-N bond construction, a C-H amination strategy could circumvent the need for prior functionalization of the arene as halide, triflate, or boronic acid. This synthetic advantage is augmented by the application of C-H amination to late-stage functionalization of synthetic targets, wherein libraries of complex aryl amines could be generated in a single step for medicinal chemistry screening.

Many of the recent advances in aryl C-H amination have been propelled by the ability of transition metals to activate C-H bonds. Although a regioselective addition to an arene that lacks a strong electronic or steric bias is an intrinsic challenge of aryl C-H functionalization, a number of researchers, including Buchwald and co-workers (*7*), Daugulis and co-workers (*8*), Shen and co-workers (*9*), and Nakamura and co-workers (*10*), have achieved orthoselective addition by relying on Lewis-basic substituents to direct the site of metalation. Beyond transition metal–catalyzed approaches, imidation of arenes and heteroarenes has been achieved by Sanford and co-workers in a photoredox mediated system (*11*), as well as by Chang (*12*) and DeBoef (*13*) and their respective co-workers, who employed $PhI(OAc)_2$ as an oxidant (Ph, phenyl; OAc, acetate). In these cases, regioselectivity was modest at best. Of the intermolecular C-H amination examples reported in the literature, few operate with the arene as a limiting reagent. Exceptional in this regard are the systems reported in studies led by Ritter (*14*), Baran (*15*), and Itami (*16*), yet each method appears to be exclusive to a single nitrogen coupling partner.

Taken together, this body of precedent research illustrates a number of remaining challenges in aryl C-H amination chemistry: (i) achievement of site-selective addition; (ii) extension of the nitrogen coupling partner beyond amides and imides, including the direct synthesis of primary anilines; and (iii) achievement of atom-economical and mild synthetic conditions. In this report, we describe our efforts to develop a C-H amination methodology that addresses these limitations and demonstrates the combination of organic photoredox catalysis with nitroxyl radicals as co-catalysts.

We hypothesized that an arene cation radical could serve as a key reactive intermediate in a direct, intermolecular C-H aryl amination. We believed that an amine could form σ-adduct **2** with an arene cation radical **1**, generated upon photoinduced electron transfer (PET) from the arene to an excited-state photoredox catalyst (cat*) (Fig. 1) (*17*–*21*). The subsequent deprotonation of distonic cation radical **2,** followed by oxidative aromatization of intermediate **3**, would deliver the desired aminated arene. As this process constitutes a two-electron and two-proton loss, an equivalent of a two-electron oxidant would be required for each photocatalyst turnover. In addition to an earlier report of an intramolecular cyclization initiated by PET (*22*), several recent investigations suggested that such a process was feasible. First, Yoshida and co-workers reported the synthesis of aryl amines by means of electrochemical oxidation (*23*–*25*). Essential to this achievement was the use of protected amines to insulate the C-N–coupled products from subsequent oxidative degradation. Accordingly, an additional synthetic step was required to liberate the desired targets. Second, Fukuzumi and co-workers studied the addition of bromide and fluoride anions to arene cation radicals, generated upon PET, via an organic photoredox catalyst (*26*, *27*). Dioxygen (O_2) served as a terminal oxidant and was believed to play a role in both the regeneration of the photoredox catalyst and the aromatization to furnish the aryl halide.

These studies lend support for the arene amination blueprint outlined in Fig. 1, and, given that aerobic conditions have been used in previous oxidative photoredox processes, O_2 was an attractive

Department of Chemistry, University of North Carolina–Chapel Hill, Chapel Hill, NC 27599-3290, USA.
***Corresponding author. E-mail: nicewicz@unc.edu**

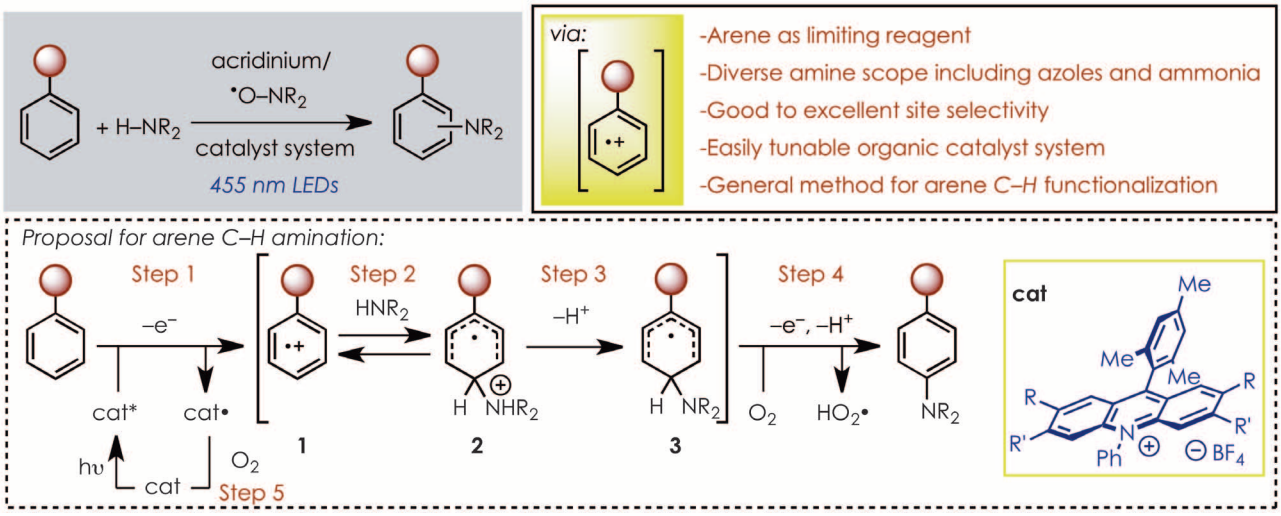

Fig. 1. A blueprint for site-selective C-H amination of aromatics. LEDs, light-emitting diodes; hυ, light.

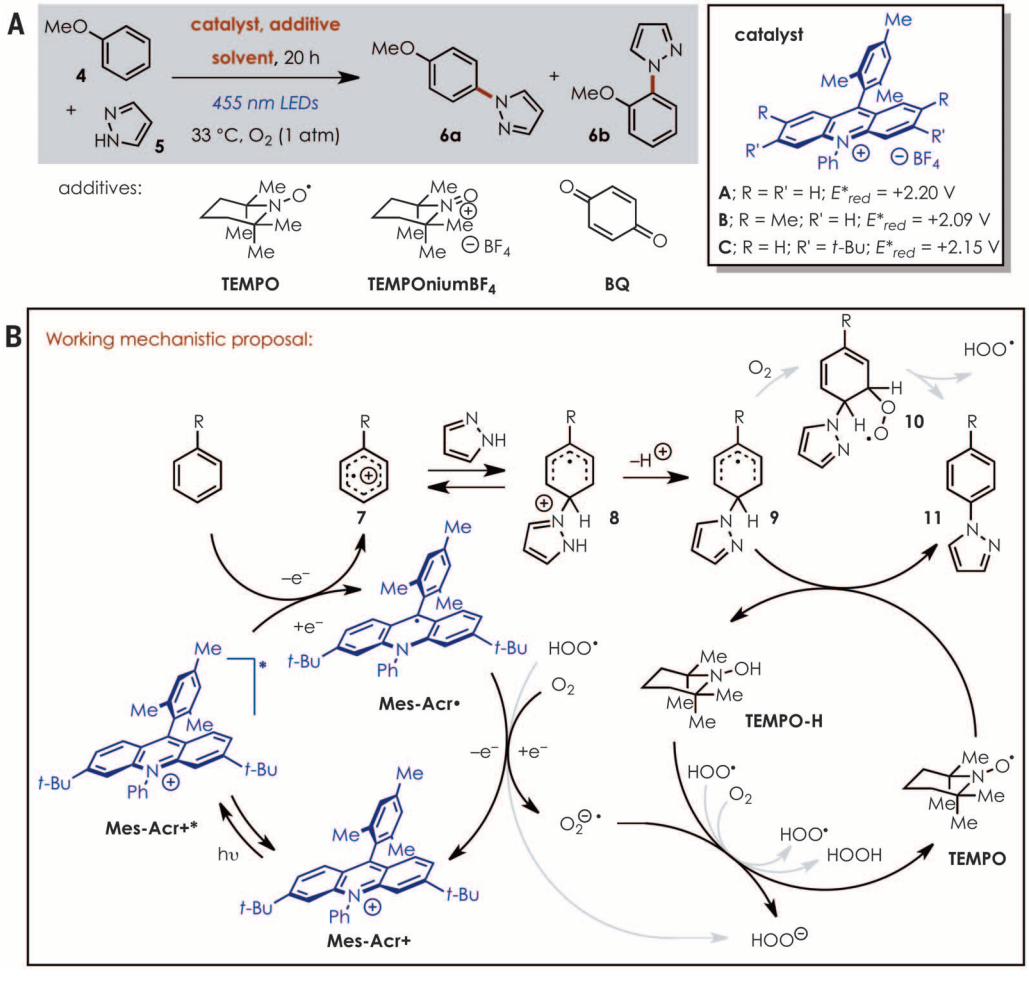

Fig. 2. Reaction development. (**A**) Catalyst optimization and (**B**) the proposed mechanism. Reactions run with 1.0 equivalent of **4** and 2.0 equivalents of **5**, unless otherwise noted. E^*_{red} values for **A** to **C** are given versus SCE (see the supplementary materials for details). BQ, 1,4-benzoquinone.

choice as a terminal oxidant and was our starting point for this investigation.

In our initial screens for reactivity, we used commercially available acridinium catalysts **A** and **B** (Fig. 2, inset), as they have highly positive excited-state reduction potentials [E^*_{red} = +2.20 and +2.09 V versus the saturated calomel electrode (SCE), respectively] and are robust in the presence of strong nucleophiles. We selected pyrazole (**5**) as a representative nucleophile and anisole (**4**) as the arene coupling partner (*28*). Under the conditions given in Fig. 2A, but in the absence of oxygen, little C-N–coupled arene adduct (**6a** and **6b**) was observed. However, when the reaction was run under a balloon of O_2, a combined 47% yield of **6a** and **6b** was observed, with good para:ortho selectivity (ratio of 6.7:1). Subsequent first-pass optimization efforts produced

no gain in yield for the catalyst, concentration, solvent, or other oxidants.

This plateau in yield could have several causes. First, aryl amine products **6a** and **6b** (irreversible half-peak potential, $E_{p/2}$ = +1.50 V versus SCE) possess lower oxidation potentials than anisole does ($E_{p/2}$ = +1.87 V versus SCE), and **6a** and **6b** could competitively reduce excited-state acridinium (cat^{+*}), resulting in product inhibition. Second, analysis of the reaction mixture revealed that phenyl formate was the major byproduct, indicating that, in addition to product inhibition, side reactions of the arene reactant were problematic under these conditions. Third, after failing to detect catalyst **A** or **B** in crude proton nuclear magnetic resonance (^{1}H NMR) spectra, we questioned the stability of the catalyst under the reaction conditions. Moreover, both anisole (**4**) and acridinium are susceptible to degradation reactions in the presence of oxygen-centered radicals (*29*); we therefore surveyed a number of additives that could mitigate any highly reactive radical intermediates, such as peroxyl radicals.

We found that 10 mol % 2,2,6,6-tetramethylpiperidine-1-oxyl (TEMPO) improved the yield of **6a** and **6b** to 65%. We also observed that the remaining mass balance was almost entirely unreacted anisole. Increased equivalents of TEMPO afforded a yield of 74% that decreased with higher loadings.

As an additional measure to prolong the viability of the acridinium catalyst, we modified the acridinium structure to confer stability against addition of nucleophiles or radicals (9-mesityl-3,6-di-*tert*-butyl-10-phenylacridinium tetrafluoroborate, **C**). The use of this catalyst provided the best results to date, producing compound **6** in 88% yield after 20 hours. A 97% yield was achieved under an atmosphere of air after irradiation for 3 days. The use of immobilized TEMPO on polystyrene resulted in a 65% yield of the aminated arene and facilitated its recovery and reuse via simple filtration.

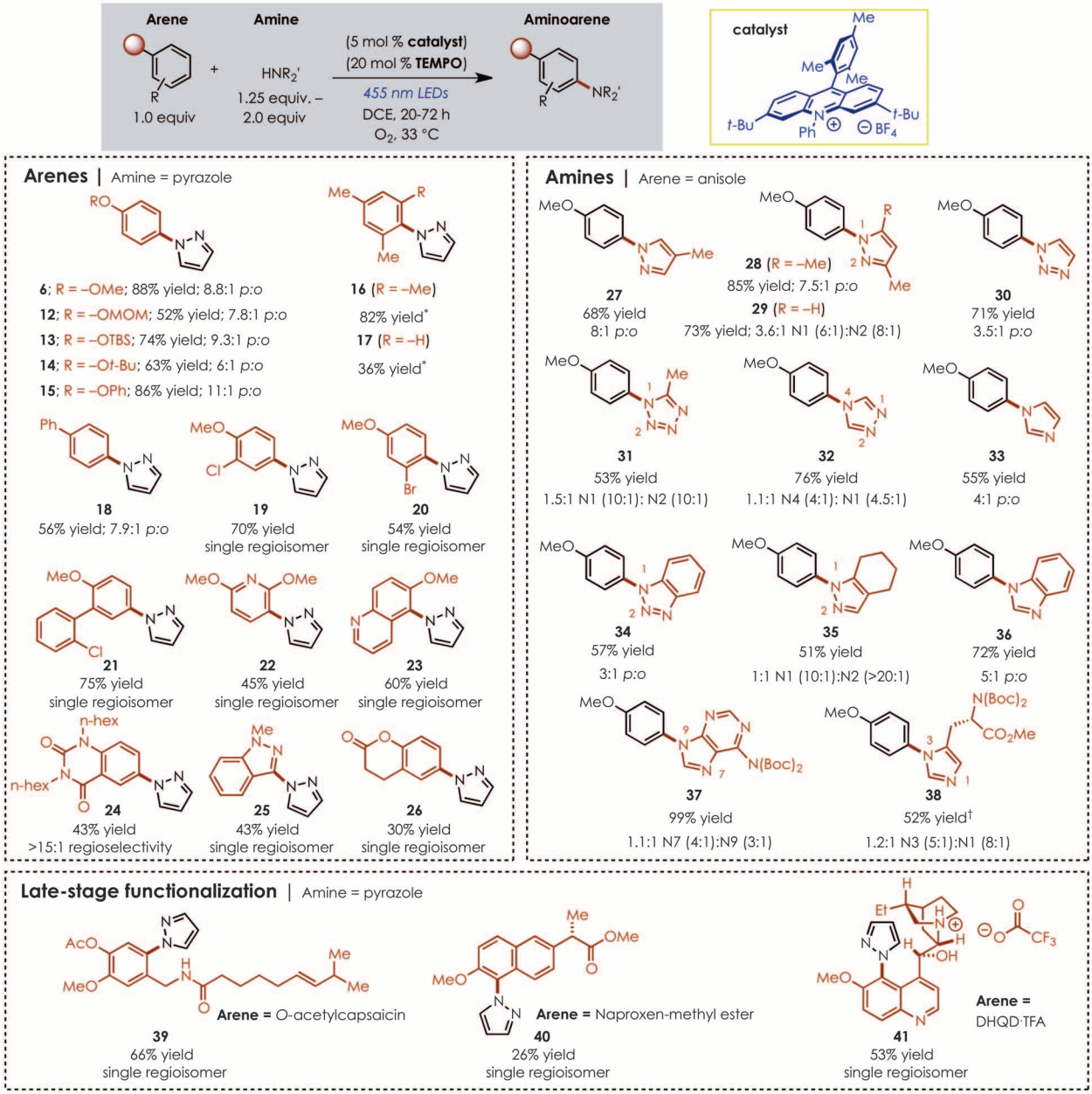

Fig. 3. Reaction scope for the C-H amination. Parenthetical ratios refer to para:ortho (p:o) selectivity for the given *N*-isomer. Reactions were run in 1,2-dichloroethane (DCE) at 0.1 M concentration with respect to the arene limiting reagent. The asterisk indicates a reaction run with 2.0 equivalents of arene, 1.0 equivalent of amine, and 1.0 equivalent of TEMPO under an N_2 atmosphere for 44 hours. The dagger indicates a reaction run under N_2 with 1.0 equivalent of TEMPO. Hex, hexyl group; Ac, acetyl group.

The mechanism of this reaction is currently the subject of detailed investigation. We believe the role of TEMPO is to aromatize radical intermediate **9** directly by H-atom abstraction (Fig. 2B). Alternatively, radical **9** could be trapped by O_2 to form 1,3-cyclohexadienyl peroxyl radical **10**, from which internal elimination would yield product **11** and hydroperoxyl radical $HO_2^{\bullet}$ (*30*). As proposed in (*26*), O_2 can oxidize acridine radical Mes-Acr• (Mes, mesityl; Acr, acridinium), regenerating acridinium Mes-Acr+ and superoxide $O_2^{-\bullet}$, although other putative intermediates might be capable of catalyst turnover (e.g., HOO•) (Fig. 2B). The strongly basic superoxide should deprotonate intermediate **10**, then undergo hydrogen atom transfer with TEMPO-H, ultimately forming H_2O_2 and regenerating TEMPO. The decrease in undesired byproducts observed when TEMPO was included is consistent with the proposed activity of TEMPO-H, which is expected to scavenge reactive oxygen-centered radicals, such as hydroperoxyl radical $HO_2^{\bullet}$. Although the half-wave redox potential of TEMPO [$E_{1/2}$ (TEMPO•/TEMPO$^+$) = +0.62 V versus Ag/AgCl] (*31*) points to the possibility of oxidization by cat^{+}*, the use of 20 mol % TEMPOnium-BF_4 produced comparable results to TEMPO in the aryl amination reaction (table S1). This suggests that a common mechanistic intermediate is accessible—namely, TEMPO—presumably generated by electron transfer from cat• ($E_{1/2}$ (cat$^+$/cat•) = −0.47 to −0.58 V versus SCE) to TEMPOnium. In the absence of cat$^+$, none of aryl amine **11** was generated with 20 mol % TEMPO, although trace product formation was detected when 20 mol % TEMPOnium-BF_4 was used and the acridinium photocatalyst was omitted.

The optimized conditions were successfully extended to the coupling of pyrazole with a variety of monosubstituted aromatics, including CH_2OCH_3 (MOM)– and *tert*-butyldimethylsilyl (TBS)–protected phenol as well as biphenyl (**12** to **15, 18**; Fig. 3). Halogenated anisole derivatives were excellent substrates for the transformation and afforded *N*-arylpyrazoles **19** and **20**, with complete regioselectivity para to the methoxy substituent. Likewise, regiochemical discrimination is possible on biaryls bearing electronically distinct aromatic groups. Despite the availability of eight unique aryl C-H bonds in 2-chloro-2'-methoxy-1,1'-biphenyl, biaryl **21** was formed in 75% yield, with completely site-selective addition para to the methoxy group, reflective of the electronic influences on this manifold. Heterocycles bearing electron-releasing substitution are competent substrates: Dimethoxypyridine **22** and methoxyquinoline **23** were isolated in modest yields but as single products. Heterocyclic motifs such as quinazoline dione, 1-methyl indazole, and dihydrocoumarin readily underwent C-H amination with pyrazole to produce adducts **24** to **26**. In all cases, a regioselectivity ratio of >15:1 was observed.

One of the challenges associated with the oxidative functionalization of arenes is the presence of weak benzylic C-H bonds, particularly in arene cation radicals, which have a documented propensity for H-atom and/or proton loss at these positions (*32*). For example, under the electrochemical oxidation conditions in (*24*), alkyl-substituted arenes give rise to benzylic amination over aryl amination. Our initial attempts to apply the previously optimized conditions to the coupling of pyrazole with mesitylene were hampered by competitive benzylic oxidation to the aryl aldehyde (table S2), a reactivity previously documented in (*33*). Excluding O_2 suppressed benzylic oxidation and increasing the TEMPO loading to 1.0 equivalent enabled the addition of pyrazole to the aromatic ring of mesitylene, forming **16** in excellent yield (82%). No products resulting from benzylic oxidation were observed. Likewise, *m*-xylene reacted under these conditions, albeit in lower yields (36%); the remainder of the mass balance was attributed to unreacted starting material. Even modest yields are notable in this context, given the oxidation potential of *m*-xylene ($E_{p/2}$ = +2.28 V versus SCE) and the excited-state reduction potential of catalyst **C**. Considering the acidity of alkylbenzene cation radicals [pK_a [PhMe]$^{+\bullet}$ = −20, where K_a is the acid dissociation constant (*34*)], it is remarkable that productive aryl C-H amination occurs for mesitylene and *m*-xylene.

Azoles are a privileged structural unit in pharmacologically active compounds (*35*, *36*) and in the architectures of transition metal–catalysts and organocatalysts. Yet the most reliable methods for constructing aryl-azoles require at least two synthetic steps. We found that a diverse range of *N*-heterocyclic nucleophiles could be directly coupled to an arene in our reaction protocol. In addition to pyrazoles (**27** to **29**), we found that 1,2,3- and 1,2,4-triazoles (**30**, **32**), tetrazole (**31**), imidazole and benzimidazole (**33** and **36**), benzotriazole (**34**), and tetrahydro-indazole (**35**) produced good to excellent yields of the C-N adducts (53 to 85%). A di-Boc–protected adenine (Boc, butoxycarbonyl) gave nearly quantitative yields (99%) of purines (**37**) in a 1.1:1 *N*-regioisomeric ratio.

To evaluate whether this catalyst system could be applied to late-stage functionalization, we tested the C-N bond–forming protocol with representative druglike molecules, as shown in Fig. 3 (bottom). The successful coupling of Boc-histidine methyl ester with **4** offers a new strategy for the modification of biologically relevant structures containing this amino acid. When reacted with pyrazole, *O*-acetylcapsaicin, naproxen methyl ester, and dihydroquinidine·trifluoroacetic acid (DHQD·TFA) were transformed into single regioisomers of the adducts (**38** to **41**). Despite heteroatom substitution at the benzylic position, no oxidation of the benzylic C-H bonds was observed in either *O*-acetylcapsaicin or DHQD·TFA in the reactions forming **39** and **41**, respectively. Likewise, naproxen methyl ester contains a sensitive benzylic C-H bond that remained undisturbed in the coupling reaction. These results demonstrate the mildness and practicality of the protocol.

The regioselectivities observed in these transformations are challenging to interpret, given the diversity of substituents on the arene coupling partner. Previous studies have found qualitative correlations between the observed site selectivity and the lowest unoccupied molecular orbital coefficients (*23*) or partial atomic charges (*26*). The aforementioned work is consistent with the expectation of nucleophilic addition to a cation radical at positions that afford a stabilized radical; in arenes bearing a single substituent, addition at the ortho and para positions is favored over meta-addition. Other differentiating factors, such as steric effects, may be intertwined with arene electronics, and future mechanistic studies could clarify the key contributions to the regioselectivities observed.

Last, we explored whether anilines could be forged directly from this catalytic sequence by using either ammonia or an ammonium salt as the nitrogen source. Traditionally, a nitration-hydrogenation sequence is used to access anilines directly. The latter protocol requires rigorous

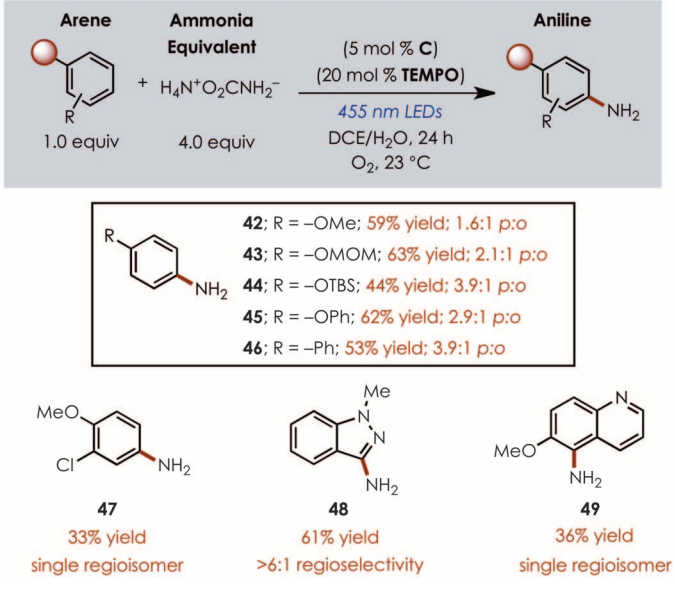

Fig. 4. Synthesis of anilines using ammonium salt as ammonia equivalent. Reactions were run in DCE and H_2O (10:1) at 0.1 M concentration with respect to the arene limiting reagent.

optimization to ensure safe dissipation of the heat associated with the exothermic reaction profile; potentially explosive intermediates and toxic byproducts are also concerns. Only recently has the Buchwald-Hartwig amination of aromatic halides been accomplished with ammonia as the nitrogen source (*37*). A C-H amination protocol of benzene with ammonia, developed by DuPont, uses a NiO-ZrO_2 catalyst system at 350°C and 300 to 400 atm, producing aniline in a 14% maximum yield (*38*, *39*).

After screening a variety of commercially available ammonium salts such as $H_4N^+OAc^-$, $H_4N^+HCO_3^-$, and $(H_4N^+)_2CO_3^{2-}$, we found that ammonium carbamate ($H_4N^+H_2NCO_2^-$) was best suited for this role (table S3 and supplementary materials). This benchtop-stable solid salt is less costly on a molar basis than liquid ammonia. Using 4.0 equivalents of ammonium carbamate with anisole, under catalytic conditions nearly identical to those applied to azoles, resulted in the formation of a 1.6:1 mixture of *para*- and *ortho*-anisidine in 59% isolated yield (**42**; Fig. 4).

The scope of the aniline-forming reaction was similar to the azole-coupling transformations. Protected phenols (**43** to **45**), haloarenes (**47**), and nitrogen heteroaromatics such as *N*-methylindazole (**48**) and 6-methoxyquinoline (**49**) were aminated under this protocol, albeit with modest regioselectivities in the case of the monosubstituted aromatics.

Overall, these C-N bond–forming reactions are powerful tools for the synthesis of complex aromatics using an organic photooxidant and nitroxyl radical catalyst system. From the substrate scope investigation, it is clear that free alcohols, esters, silyl ethers, halides, amides, alkenes, and protected amines are all compatible functionalities. The mildness of this protocol makes it appealing for a variety of applications. Moreover, we anticipate that this general method for the activation of arenes will result in the development of additional transformations.

REFERENCES AND NOTES

1. T. W. Lyons, M. S. Sanford, *Chem. Rev.* **110**, 1147–1169 (2010).
2. G. B. Shul'Pin, in *Transition Metals for Organic Synthesis: Building Blocks and Fine Chemicals*, M. Beller, C. Bolm, Eds. (Wiley-VCH, New York, ed. 2, 2004), pp. 215–241.
3. J. P. Wolfe, S. Wagaw, J.-F. Marcoux, S. L. Buchwald, *Acc. Chem. Res.* **31**, 805–818 (1998).
4. J. F. Hartwig, *Acc. Chem. Res.* **31**, 852–860 (1998).
5. P. Y. S. Lam, G. Vincent, C. G. Clark, S. Deudon, P. K. Jadhav, *Tetrahedron Lett.* **42**, 3415–3418 (2001).
6. K. Sanjeeva Rao, T.-S. Wu, *Tetrahedron* **68**, 7735–7754 (2012).
7. W. C. P. Tsang, R. H. Munday, G. Brasche, N. Zheng, S. L. Buchwald, *J. Org. Chem.* **73**, 7603–7610 (2008).
8. L. D. Tran, J. Roane, O. Daugulis, *Angew. Chem. Int. Ed.* **52**, 6043–6046 (2013).
9. H. Xu, X. Qiao, S. Yang, Z. Shen, *J. Org. Chem.* **79**, 4414–4422 (2014).
10. T. Matsubara, S. Asako, L. Ilies, E. Nakamura, *J. Am. Chem. Soc.* **136**, 646–649 (2014).
11. L. J. Allen, P. J. Cabrera, M. Lee, M. S. Sanford, *J. Am. Chem. Soc.* **136**, 5607–5610 (2014).
12. H. J. Kim, J. Kim, S. H. Cho, S. Chang, *J. Am. Chem. Soc.* **133**, 16382–16385 (2011).
13. A. A. Kantak, S. Potavathri, R. A. Barham, K. M. Romano, B. DeBoef, *J. Am. Chem. Soc.* **133**, 19960–19965 (2011).
14. G. B. Boursalian, M.-Y. Ngai, K. N. Hojczyk, T. Ritter, *J. Am. Chem. Soc.* **135**, 13278–13281 (2013).
15. K. Foo, E. Sella, I. Thomé, M. D. Eastgate, P. S. Baran, *J. Am. Chem. Soc.* **136**, 5279–5282 (2014).
16. T. Kawakami, K. Murakami, K. Itami, *J. Am. Chem. Soc.* **137**, 2460–2463 (2015).
17. C. K. Prier, D. A. Rankic, D. W. C. MacMillan, *Chem. Rev.* **113**, 5322–5363 (2013).
18. J. M. R. Narayanam, C. R. J. Stephenson, *Chem. Soc. Rev.* **40**, 102–113 (2011).
19. D. A. Nicewicz, T. M. Nguyen, *ACS Catal.* **4**, 355–360 (2014).
20. Q. Qin, S. Yu, *Org. Lett.* **16**, 3504–3507 (2014).
21. E. Brachet, T. Ghosh, I. Ghosh, B. König, *Chem. Sci.* **6**, 987–992 (2015).
22. G. Pandey, M. Sridhar, U. T. Bhalerao, *Tetrahedron Lett.* **31**, 5373–5376 (1990).
23. T. Morofuji, A. Shimizu, J. Yoshida, *J. Am. Chem. Soc.* **135**, 5000–5003 (2013).
24. T. Morofuji, A. Shimizu, J. Yoshida, *J. Am. Chem. Soc.* **136**, 4496–4499 (2014).
25. T. Morofuji, A. Shimizu, J. Yoshida, *Chem. Eur. J.* **21**, 3211–3214 (2015).
26. K. Ohkubo, K. Mizushima, R. Iwata, S. Fukuzumi, *Chem. Sci.* **2**, 715–722 (2011).
27. K. Ohkubo, A. Fujimoto, S. Fukuzumi, *J. Phys. Chem. A* **117**, 10719–10725 (2013).
28. T. M. Nguyen, N. Manohar, D. A. Nicewicz, *Angew. Chem. Int. Ed.* **53**, 6198–6201 (2014).
29. W. P. Hess, F. P. Tully, *J. Phys. Chem.* **93**, 1944–1947 (1989).
30. X.-M. Pan, M. N. Schuchmann, C. von Sonntag, *J. Chem. Soc. Perkin Trans. 2* **1993**, 289–297 (1993).
31. J. E. Baur, S. Wang, M. C. Brandt, *Anal. Chem.* **68**, 3815–3821 (1996).
32. M. Schmittel, A. Burghart, *Angew. Chem. Int. Ed. Engl.* **36**, 2550–2589 (1997).
33. K. Ohkubo *et al.*, *Chem. Commun. (Cambridge)* **46**, 601–603 (2010).
34. F. G. Bordwell, J. P. Cheng, *J. Am. Chem. Soc.* **111**, 1792–1795 (1989).
35. E. Vitaku, D. T. Smith, J. T. Njardarson, *J. Med. Chem.* **57**, 10257–10274 (2014).
36. T. J. Ritchie, S. J. F. Macdonald, S. Peace, S. D. Pickett, C. N. Luscombe, *Med. Chem. Comm.* **3**, 1062–1069 (2012).
37. G. D. Vo, J. F. Hartwig, *J. Am. Chem. Soc.* **131**, 11049–11061 (2009).
38. T. W. Del Pesco, U.S. Patent 4031106 (1977).
39. T. W. Del Pesco, U.S. Patent 4001260 (1977).

ACKNOWLEDGMENTS

Financial support was provided by the David and Lucile Packard Foundation, Merck, and an Amgen Young Investigator Award. N.A.R is grateful for an NSF Graduate Fellowship, and K.A.M. was supported by a Francis Preston Venable Graduate Fellowship. A provisional patent has been filed on the methods presented here (U.S. patent application no. 62/170,632).

SUPPLEMENTARY MATERIALS

www.sciencemag.org/content/349/6254/1326/suppl/DC1
Materials and Methods
Tables S1 to S4
References (*40*–*73*)
NMR Spectra

9 July 2015; accepted 19 August 2015
10.1126/science.aac9895

MINERAL SURFACES

X-ray–driven reaction front dynamics at calcite-water interfaces

Nouamane Laanait,[1,2]*† Erika B. R. Callagon,[2,3] Zhan Zhang,[4] Neil C. Sturchio,[5] Sang Soo Lee,[1] Paul Fenter[1]*

The interface between minerals and aqueous solutions hosts globally important biogeochemical processes such as the growth and dissolution of carbonate minerals. Understanding such processes requires spatially and temporally resolved observations and experimental controls that precisely manipulate the interfacial thermodynamic state. Using the intense radiation fields of a focused synchrotron x-ray beam, we drove dissolution at the calcite/water interface and simultaneously probed the dynamics of the propagating reaction fronts using surface x-ray microscopy. Evolving surface structures were controlled by the time-dependent solution composition, as characterized by a kinetic reaction model. At extreme disequilibria, we observed the onset of reaction front instabilities with velocities of > 30 nanometers per second. These instabilities serve as a signature of transport-limited dissolution of calcite under extreme disequilibrium.

Calcium carbonate precipitates abiotically and is synthesized by living organisms into complex and functional biomineral architectures (*1*). Combined, calcium carbonate minerals constitute a major fraction of Earth's upper crust in the form of carbonate rocks (*2*). Characterizing the rapidly evolving morphology of calcium carbonate during growth (*3*, *4*) and dissolution (*5*, *6*) is central to both a fundamental understanding of its reactivity and manipulation of its versatile functionality. The morphology of calcium carbonate phases can be imaged in situ with electron (*7*, *8*) and x-ray microscopies; however, the large radiation doses deposited by these probes can substantially alter the state of the system (*9*).

We used a focused x-ray beam to both observe and drive dissolution in a quantifiable manner (*10*). The synchrotron x-ray beam induces acidification and depletion of carbonate ions within the solution, which controlled the interfacial

[1]Chemical Sciences and Engineering Division, Argonne National Laboratory, Argonne, IL, USA. [2]Center for Nanophase Materials Sciences, Oak Ridge National Laboratory, Oak Ridge, TN, USA. [3]Department of Earth and Environmental Sciences, University of Illinois at Chicago, Chicago, IL, USA. [4]X-ray Science Division, Argonne National Laboratory, Argonne, IL, USA. [5]Department of Geological Sciences, University of Delaware, Newark, DE, USA.
***Corresponding author. E-mail: laanaitn@ornl.gov (N.L.); fenter@anl.gov (P.F.)** †Present address: Center for Nanophase Materials Sciences, Oak Ridge National Laboratory, Oak Ridge, TN, USA.